ELSEVIER

Journal of Photochemistry and Photobiology A: Chemistry 109 (1997) 53–57

Journal of PHOTOCHEMISTRY AND PHOTOBIOLOGY A:CHEMISTRY

Absorption and fluorescence spectroscopic analysis of rhodamine 6G and oxazine 750 in porous sol–gel glasses

P. Sathy [1], A. Penzkofer *

Naturwissenschaftliche Fakultät II–Physik, Universität Regensburg, D-93040 Regensburg, Germany

Received 15 July 1996; accepted 12 March 1997

Abstract

The absorption cross-section spectra, stimulated emission cross-section spectra, fluorescence quantum yields and degrees of fluorescence polarisation of the dyes rhodamine 6G and oxazine 750 in porous silicate sol–gel glasses and in methanol are determined. Gelsil glasses of 2.5 nm, 5 nm, and 7.5 nm pore diameter are studied. For the investigated pore size range the absorption and emission spectroscopic parameters are independent of the pore size. Some concentration dependent effects are observed on the Gelsil glass fluorescence spectra due to chemisorption and physisorption. © 1997 Elsevier Science S.A.

Keywords: Dye-doped sol-gel glasses; Gelsil; Rhodamine 6G; Oxazine 750; Fluorescence quantum yield

1. Introduction

Dye-doped sol–gel glasses are used as laser media [1,2], non-linear optical materials [3,4] and optical sensors [3,4]. Spectroscopic studies of coloured sol–gel glasses have been performed [5,6].

In this paper three silicate sol–gel glasses (Gelsil from Geltech [7]) of average pore diameter of 2.5 nm (Gelsil 25), 5 nm (Gelsil 50), and 7.5 nm (Gelsil 75) have been doped with rhodamine 6G and oxazine 750. The absorption and emission spectroscopic behaviour of the dye-doped glasses is compared with methanolic solutions. The absorption and emission spectra, the fluorescence quantum yields, and the degrees of fluorescence polarisation are found to be independent of the pore size in the investigated range. The fluorescence studies indicate a concentration dependent change from chemisorption to physisorption.

2. Experimental

The porous silicate sol–gel glasses were purchased from Geltech [7]. The porosity and density parameters are listed in Table 1 (from Ref. [7]). The size of the disks was 1 cm diameter and 5 mm thickness. The dyes were purchased from Lambda Physik and used without further purification. The porous glasses were doped with dye by bringing the samples into bottles with methanolic dye solution and putting the samples into an ultrasonic bath. Then the solvent was slowly evaporated in a heating chamber by rising the temperature to 70 °C. Finally the temperature was increased shortly to 110 °C to remove any water content. The samples are kept in a desiccator. The dye penetration rate decreases with decreasing pore size. For Gelsil 75 a homogeneous dye distribution was achieved after 6 h of ultrasonic shaking, for Gelsil 50 an ultrasonic shaking of about 12 h was needed, while for Gelsil 25 about 24 h of ultrasonic shaking resulted in a nearly homogeneous dye distribution.

The absorption cross-section spectra are determined by transmission measurements with a commercial spectro-photometer (Beckman ACTA M4). The fluorescence measurements are performed with a self-assembled fluorometer [8] using the front-face fluorescence collection technique. Rhodamine 6G in methanol is used as reference dye for the rhodamine 6G doped samples (fluorescence quantum yield $\phi_R = 0.90$ [9]), and rhodamine 800 in methanol is used as reference dye for the oxazine 750 doped samples ($\phi_R = 0.16$ [10]). The degree of fluorescence polarisation of the samples, $P_F = (S_\parallel - S_\perp)/(S_\parallel + S_\perp)$, where $S_\parallel$ ($S_\perp$) is the fluorescence signal polarised parallel (perpendicular) to the excitation light, is normalised to the degree of fluorescence polarisation of the reference dyes. P_F of the reference dyes is calculated from the reorientation time, τ_{or}, and fluorescence lifetime, τ_F, using the relation [11]

* Corresponding author.

[1] Deceased on 4 December 1995 in Cochin, Kerala, India.

PII S1010-6030(97)00104-4

Table 1
Parameters of porous glasses and dye doped samples at room temperature

	Gelsil 25	Gelsil 50		Gelsil 75		Methanol
Pore diameter d_p (nm) [a]	2.5	5.0		7.5		
Porosity p [a]	0.48	0.63		≈ 0.7		
Density ρ (g cm^{-3}) [a]	1.2	0.9		≈ 0.7		
Specific surface S (m^2 g^{-1}) [a]	610	580		525		
Chemisorption sites N_{ch} (g^{-1}) [b]	$\approx 4\times10^{17}$	$\approx 1.1\times10^{17}$				
Dopand rhodamine 6G						
n_a [c]	1.2284	1.1574		1.1267		1.331 [d]
n_{em} [c]	1.2241	1.1569		1.1263		1.330 [d]
C (mol dm^{-3})	2×10^{-4}	2×10^{-4}		4×10^{-5}	2×10^{-4}	1×10^{-5}
N_{ad} (g^{-1})	1×10^{17}	1.3×10^{17}		$\approx 3.4\times10^{16}$	$\approx 1.7\times10^{17}$	
ϕ_F	0.79 ± 0.1	0.72 ± 0.1		0.7 ± 0.1	0.75 ± 0.1	0.9 [e]
P_F	0.27 ± 0.03	0.30 ± 0.03		0.41 ± 0.03	0.31 ± 0.03	0.025
τ_{rad} (ns)	5.1	5.6		5.7	6.0	4.3
τ_F (ns)	4.0	4.0		4.0	4.5	3.9 [f]
τ_{or} (ns)	3.9	5.0		15	6.1	0.17 [g]
Dopand oxazine 750						
n_a [c]	1.2227	1.156		1.1256		1.3277 [d]
n_{em} [c]	1.2221	1.1555		1.1253		1.3273 [d]
C (mol dm^{-3})	4.9×10^{-5}	2.5×10^{-5}	6×10^{-5}	1.7×10^{-5}	6.6×10^{-5}	1×10^{-5}
N_{ad} (g^{-1})	2.5×10^{16}	1.7×10^{16}	4×10^{16}	$\approx 1.5\times10^{16}$	$\approx 5.7\times10^{16}$	
ϕ_F	0.17 ± 0.02	0.18 ± 0.02	0.15 ± 0.02	0.15 ± 0.02	0.15 ± 0.02	0.15 ± 0.02
P_F	0.44 ± 0.04	0.47 ± 0.02	0.47 ± 0.02	0.49 ± 0.03	0.47 ± 0.03	0.091
τ_{rad} (ns)	7.1	7.9	8.1	8.5	8.6	6.6
τ_F (ns)	1.2	1.4	1.2	1.3	1.3	1.0
τ_{or} (ns)	7.3	18.3	15.7	53	17	0.15

[a] Ref. [7].
[b] Ref. [21].
[c] From the Clausius Mossotti relation $(n^2-1)/(n^2+2)=(1-\rho)(n_0^2-1)/(n_0^2+1)$ [22], where n_0 is the refractive index of fused silica [23]; n_a, the average refractive index in the S_0–S_1 absorption band; n_{em}, the average refractive index in the S_1–S_0 emission band.
[d] Ref. [23].
[e] Ref. [9].
[f] Ref. [12].
[g] Ref. [13].

$$\left(\frac{1}{P_F}-\frac{1}{3}\right)=\left(\frac{1}{P_{F,0}}-\frac{1}{3}\right)\left(1+\frac{\tau_F}{\tau_{or}}\right) \quad (1)$$

with $P_{F,0}=0.5$. For rhodamine 6G in methanol the used parameters are $\tau_F=3.9$ ns [12] and $\tau_{or}=170$ ps [13] giving $P_F=0.025$. For rhodamine 800 in methanol the used parameters are $\tau_F=1.54$ ns [10] and $\tau_{or}=150$ ps (assumed) giving $P_F=0.05$.

3. Results

3.1. Absorption studies

The absorption cross-section spectrum of rhodamine 6G in Gelsil 75 is shown in Fig. 1(a). The S_0–S_1 absorption peak was measured with a sample of $C=2.5\times10^{-5}$ mol dm^{-3} dye concentration and the rest of the spectrum was measured with a sample of $C=2\times10^{-4}$ mol dm^{-3} dye concentration. For comparison the absorption cross-section spectrum of rhodamine 6G in methanol is displayed in Fig. 1(b). The spectrum of rhodamine 6G in Gelsil 75 is slightly broader and

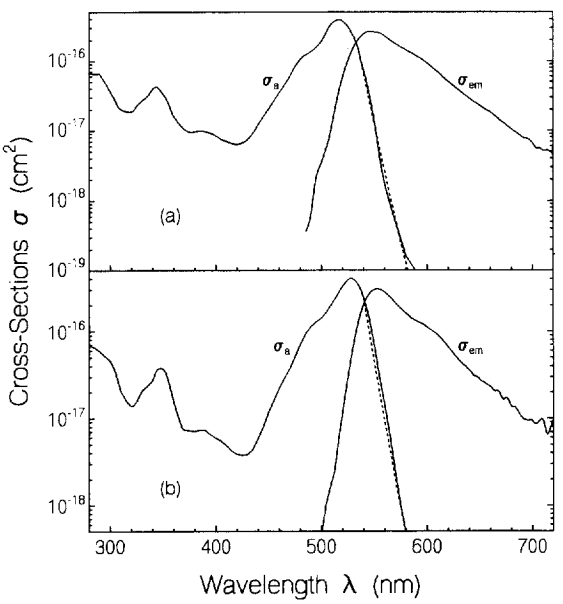

Fig. 1. Absorption cross-section and stimulated emission cross-section spectra of rhodamine 6G in Gelsil 75 (a) and rhodamine 6G in methanol (b). · · ·, theoretical thermal population curve. Low concentration data are used.

shifted by 10 nm to shorter wavelengths compared to the spectrum of rhodamine 6G in methanol (S_0–S_1 absorption peak at $\lambda_{max} = 517$ nm for the Gelsil sample and at $\lambda_{max} = 528$ nm for the methanolic sample). The experimentally determined S_0–S_1 absorption cross-section integral of rhodamine 6G in the sol–gel glass and in methanol were found to be roughly equal. In Fig. 1 the absorption cross-section integral of rhodamine 6G in sol–gel glass is made equal to the value of rhodamine 6G in methanol. The dotted lines indicate the expected long-wavelength absorption cross-section slope for the thermal S_0 ground state level population assuming a constant Franck–Condon S_0–S_1 state overlap in the displayed long-wavelength region. The dotted curves are determined by [14]

$$\sigma_a(\lambda) = \sigma_a(\lambda_0) \exp\left[\frac{-hc_0(\lambda_0^{-1} - \lambda^{-1})}{k_B \vartheta}\right] \quad (2)$$

where λ_0 is a reference wavelength around the zero vibronic S_0–S_1 transition, h is the Planck constant, c_0 is the velocity of light in vacuum, k_B is the Boltzmann constant, and ϑ is the temperature. The experimental long-wavelength slopes fit well to the expected thermal slopes. The absorption cross-section spectra of rhodamine 6G in Gelsil 50 and Gelsil 25 coincide with the displayed Gelsil 75 curve within our experimental accuracy (no curves shown).

The absorption cross-section spectrum of oxazine 750 in Gelsil 75 is shown in Fig. 2(a) (S_0–S_1 absorption peak measured with a sample of $C = 2.5 \times 10^{-5}$ mol dm^{-3}, other wavelength range measured with a sample of $C = 10^{-4}$ mol dm^{-3}). The absorption cross-section spectrum of oxazine 750 in methanol is displayed in Fig. 2(b). The S_0–S_1 absorption cross-section integral of the sol–gel sample is made equal to the S_0–S_1 absorption cross-section integral of the methanolic sample. The spectral shapes are similar. The S_0–S_1 absorption peak in the sol–gel glass sample is at 655 nm, and in methanol it is at 660 nm. The long-wavelength slope of the absorption cross-section spectrum of oxazine 750 in methanol follows the thermal population dependence of Eq. (1) (dotted curve). For oxazine 750 in Gelsil 75 some spectral broadening (inhomogeneous broadening) is observed in the long-wavelength region. The absorption cross-section spectra obtained for oxazine 750 in Gelsil 50 and Gelsil 25 are found to be the same as the displayed Gelsil 75 spectrum within our experimental accuracy (curves not shown).

3.2. Fluorescence studies

The measured fluorescence quantum distributions, $E_F(\lambda)$, for rhodamine 6G and oxazine 750 are displayed in Figs. 3 and 4, respectively. The obtained fluorescence quantum yields, $\phi_F = \int E_F(\lambda)\, d\lambda$, the degrees of fluorescence polarisation, P_F, the radiative lifetimes, τ_{rad}, the fluorescence lifetimes, $\tau_F = \phi_F \tau_{rad}$, and the molecular reorientation times, τ_{or}, are listed in Table 1. The radiative lifetimes are calculated by application of the Strickler–Berg formula [15,16]

$$\frac{1}{\tau_{rad}} = 8\pi c_0 \frac{\int_{em} E_F(\lambda)\, d\lambda}{\int_{em} E_F(\lambda)\lambda^3 n^{-3}(\lambda)\, d\lambda} \int_{abs} \frac{\sigma_a(\lambda)}{\lambda n(\lambda)}\, d\lambda \quad (3)$$

where n is the refractive index. The integrations extend over the $S_1 \rightarrow S_0$ fluorescence region (em) and the $S_0 \rightarrow S_1$ absorption region (abs). The molecular reorientation times are calculated by the relation

$$\tau_{or} = P_F \tau_F \frac{1/P_{F,0} - 1/3}{1 - P_F/P_{F,0}} \quad (4)$$

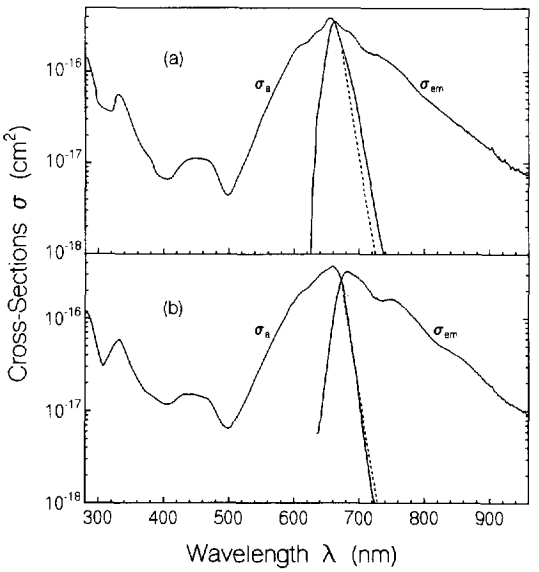

Fig. 2. Absorption cross-section and stimulated emission cross-section spectra of oxazine 750 in Gelsil 75 (a) and oxazine 750 in methanol (b). · · ·, theoretical thermal population curve. Low concentration data are used.

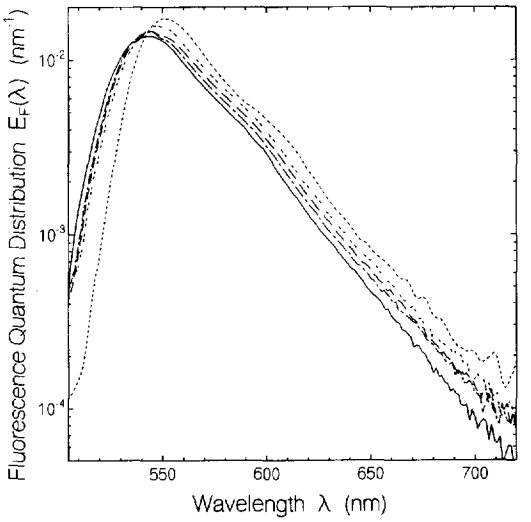

Fig. 3. Fluorescence quantum distributions of rhodamine 6G. ———, 4×10^{-5} molar in Gelsil 75; - - -, 2×10^{-4} molar in Gelsil 75; – · –, 2×10^{-4} molar in Gelsil 50; – –, 2×10^{-4} molar in Gelsil 25; · · ·, 1×10^{-5} molar in methanol.

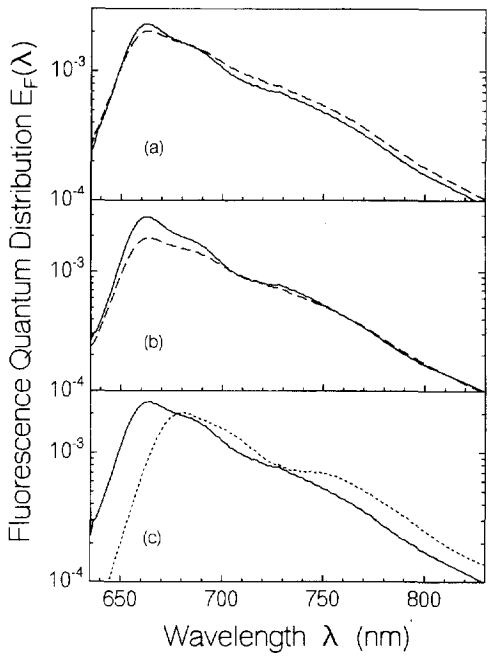

Fig. 4. Fluorescence quantum distribution of oxazine 750. (a) Gelsil 75: ———, $C=1.7\times10^{-5}$ mol dm^{-3}; - - -, $C=6.6\times10^{-5}$ mol dm^{-3}. (b) Gelsil 50: ———, $C=2.5\times10^{-5}$ mol dm^{-3}; - - -, $C=6\times10^{-5}$ mol dm^{-3}. (c) ———, 4.9×10^{-5} molar dye in Gelsil 25; · · ·, 1×10^{-5} molar dye in methanol.

which is obtained by rewriting Eq. (1). The stimulated emission cross-section spectra are included in Figs. 1 and 2. They are calculated from the fluorescence quantum distribution and the radiative lifetime by the relation [17]

$$\sigma_{em}(\lambda)=\frac{\lambda^4}{8\pi c_0 n^2(\lambda)\tau_{rad}}\frac{E_F(\lambda)}{\int_{em}E_F(\lambda)\,d\lambda} \quad (5)$$

Fluorescence quantum distributions of rhodamine 6G are displayed in Fig. 3. Curves are shown for Gelsil 75 (solid curve, $C=4\times10^{-5}$ mol dm^{-3}; dashed curve, $C=2\times10^{-4}$ mol dm^{-3}), Gelsil 50 (dash–dotted curve, $C=2\times10^{-4}$ mol dm^{-3}), Gelsil 25 (double-dashed curve, $C=2\times10^{-4}$ mol dm^{-3}), and methanol (dotted curve, $C=10^{-5}$ mol dm^{-3}). The spectral shapes of the Gelsil and methanol samples are similar. Around the emission peak the porous glass spectra are slightly more structured than the methanolic spectrum. The Gelsil sample with the lowest dye concentration (Gelsil 75, $C=4\times10^{-5}$ mol dm^{-3}) gives the steepest long-wavelength fluorescence decay.

The fluorescence quantum yield, ϕ_F, is somewhat lower in the sol–gel glasses compared to methanol. The radiative lifetimes, τ_{rad}, are larger in the sol–gel glasses than in methanol because of the reduced refractive index in the porous glasses (Eq. (3)). The degree of fluorescence polarisation, P_F, is much larger in the sol–gel glasses than in the methanolic solution. The obtained reorientation times, τ_{or}, are in the nanosecond region. They indicate a restricted motion of the dye molecules by adsorption to the pore walls. The sample with the lowest dye concentration gives the largest degree of fluorescence polarisation and the largest molecular reorientation time.

Fluorescence quantum distributions, $E_F(\lambda)$, of oxazine 750 in Gelsil 75 (a), Gelsil 50 (b), Gelsil 25 and methanol (c) are displayed in Fig. 4. At low dye concentration (solid curves in (a) and (b)) the fluorescence spectra of the Gelsil samples are sharper than the fluorescence spectrum of the methanolic sample. At high dye concentration (dashed curves in (a) and (b)) the fluorescence spectra of the Gelsil samples become broadened. The shapes of the fluorescence spectra the of the Gelsil 25 sample were found to be site dependent. The spectral peak position varied in the range from 675 nm to 683 nm at different locations (excitation spotsize was approximately 0.3 mm).

The fluorescence quantum yields, ϕ_F, of oxazine 750 in the sol–gel glasses are similar to the fluorescence quantum yield of oxazine 750 in methanol. They are independent of pore size within our experimental accuracy. The degree of fluorescence polarisation of oxazine 750 in the Gelsil glasses is rather high (theoretical limit is $P_F=0.5$ for $\tau_{or}=\infty$).

4. Discussion

For both dyes the pure electronic S_0–S_1 transition wavenumber (position where σ_a and σ_{em} are equal) is shifted approximately 200 cm^{-1} to higher wavenumbers in the porous glasses compared to the methanolic samples. This behaviour is in agreement with a solvent induced spectral shift due to dispersion force interaction which is proportional to $(n^2-1)/(2n^2+1)$ [18,19].

The spectral shapes of the fluorescence quantum distributions of rhodamine 6G and oxazine 750 in the porous Gelsil samples have been found to be concentration dependent. A specific pore size dependence could not be resolved. The specific number densities of adsorbed dye molecules [20], $N_{ad}=CN_A/(1000\rho)$ (C, concentration in mol dm^{-3}; $N_A=6.022045\times10^{23}$ mol^{-1} is the Avogadro constant; ρ is the mass density in g cm^{-3}) of the studied samples are listed in Table 1. These number densities are less or comparable to the number densities of chemisorption sites, N_{ch}, of the applied Gelsil glasses [21]. At low dye concentration the most strongly binding chemisorption sites will be occupied leading to sharpened fluorescence spectra. With rising dye concentration different chemisorption sites will be occupied and physisorption will start to occur. The concentration dependent change of adsorption strength leads to increased inhomogeneous broadening with rising dye concentration.

The chemisorption hinders rotational molecular motion. The molecular reorientation time becomes long and the degree of fluorescence polarisation becomes large. The experimental results indicate a decrease of molecular reorientation time with rising dye concentration.

5. Conclusions

A comparative absorption and emission spectroscopic study of two organic dyes in silicate sol–gel glasses of different pore size and in methanol have been performed. Within the available pore diameter range from 2.5 nm to 7.5 nm no pore size dependence has been observed. The spectral shapes of the fluorescence spectra of the dye doped Gelsil glasses were found to be concentration dependent. They indicate at low dye concentration an adsorption to chemisorption sites of highest chemical binding, followed by adsorption to less strongly binding chemisorption sites and a change over to physisorption.

Acknowledgements

The authors thank W. Holzer for experimental assistance.

References

[1] R. Reisfeld, J. Non-Cryst. Solids 121 (1990) 254.
[2] E.T. Knobbe, B. Dunn, P.D. Fugua, F. Nishida, Appl. Opt. 29 (1990) 2723.
[3] M. Canva, P. Georges, G. Le Saux, A. Brun, F. Chaput, J.P. Boilot, J. Non-Cryst. Solids 147–148 (1992) 627.
[4] R. Reisfeld, SPIE 1328 (1990) 29.
[5] D. Lo, J.E. Parris, J.L. Lawless, Appl. Phys. B55 (1992) 365.
[6] F. Ammer, A. Penzkofer, P. Weidner, Chem. Phys. 192 (1995) 325.
[7] Gelsil Porous Glass and Lenses, data sheet, Geltech, Alachua, FL 33615.
[8] A. Penzkofer, W. Leupacher, J. Luminesc. 37 (1987) 61.
[9] K.A. Selanger, J. Falnes, T. Sikkeland, J. Phys. Chem. 81 (1977) 1960.
[10] P. Sperber, W. Spangler, B. Meier, A. Penzkofer, Opt. Quantum Electron. 20 (1988) 395.
[11] C.A. Parker, Photoluminescence of Solutions, Elsevier, Amsterdam, 1968.
[12] R. Reisfeld, R. Zusman, Y. Cohen, M. Eyal, Chem. Phys. Lett. 147 (1988) 145.
[13] H.E. Lessing, A. von Jena, in: M.L. Stitch (ed.), Laser Handbook, Vol. 3, North-Holland, Amsterdam, 1979, p. 753.
[14] P. Weidner, A. Penzkofer, Chem. Phys. 191 (1995) 303
[15] S.J. Stickler, R.A. Berg, J. Chem. Phys. 37 (1962) 814.
[16] J.B. Birks, D.J. Dyson, Proc. Roy. Soc. A275 (1963) 135.
[17] O.G. Peterson, J.P. Webb, W.C. McColgin, J.H. Eberly, J. Appl. Phys. 42 (1971) 1917.
[18] M. Magata, T. Kubota, Molecular Interaction and Electronic Spectra, Dekker, New York, 1970, p. 371.
[19] A.V. Deshpande, A. Beidoun, A. Penzkofer, G. Wagenblast, Chem. Phys. 148 (1990) 141.
[20] S. Lowell, J.E. Shields, Powder Surface Area and Porosity, 3rd edn., Chapman and Hall, London, 1991.
[21] A. Penzkofer, H. Gratz, P. Weidner, J. Non-Cryst. Solids 189 (1995) 55.
[22] H. Gratz, A. Penzkofer, P. Weidner, J. Non-Cryst. Solids 189 (1995) 50.
[23] S.S. Ballard, J.S. Browder, J.F. Ebersole, in: D.E. Gray (ed.), American Institute of Physics Handbook, 3rd edn., McGraw-Hill, New York, 1972, p. 6–12.